Asian Journal of Civil Engineering
https://doi.org/10.1007/s42107-025-01444-2

RESEARCH

Pi Distribution method for numerical fracture analysis of reinforced concretes (RC) based recycled aggregates

Meryem Charef[1] · **Nabil Kazi Tani**[1,2] · **Hasan Dilbas**[3]

Received: 29 May 2025 / Accepted: 13 July 2025
© The Author(s), under exclusive licence to Springer Nature Switzerland AG 2025

Abstract

A numerical investigation was carried out for both cases of cracked and uncracked reinforced (RC) and fibrous reinforced (FRC) /unfibrous concrete specimens incorporating recycled aggregate (RA), which were assessed to explore the failure properties of these materials, using the "Pi Distribution Method" (PDM). PDM is based on the non-random distribution of aggregates, which depends on the falling aggregate experiment. A finite element (FE) software (ABAQUS) is used to model the concrete specimens. The results demonstrate an improvement in the mechanical properties of concrete after adding RA. The incorporation of RA into the concrete results in an increase in elasticity and greater displacement at loading due to their important ductility, high porosity, and weak bond to the cement matrix. RA contributes to enhancing post-cracking behavior and stress redistribution. The elastic behavior of RA concrete shows a more horizontal load-displacement curve, indicating its deformability. Both concrete reinforcements, by bars and fibers, are analyzed in terms of Load-Displacement and load-CMOD (Crack Mouth Opening Displacement) for the notched specimen. The addition of steel fibers to RA contributes to the increase of the linear elastic stiffness before and at the maximal force of the specimens by acting as dispersed reinforcement. The efficiency of the proposed numerical FE mesoscopic model based on PDM is confirmed for all the study cases. This study opens new paths in the literature, explores many types of recycled aggregates and various fiber types, and considers other structural elements as beams, columns, and joints.

Keywords Reinforced concrete · Recycled aggregates · Notch · Pi Distribution method · Mesoscopic modelling · Load-displacement · Load-CMOD

Abbreviations

RC	Reinforced Concrete
FRC	Fiber-Reinforced Concrete
RA	Recycled Aggregates
PDM	Pi Distribution Method
FE	Finite Element
CMOD	Crack Mouth Opening Displacement
RCA	Recycled Concrete Aggregate
NA	Natural Aggregates

✉ Meryem Charef
charefmeryem13@gmail.com

Nabil Kazi Tani
kazitani_nabil@yahoo.fr

Hasan Dilbas
hasandilbas@gmail.com

[1] RISAM Laboratory, Department of Civil Engineering, Faculty of Technology, University of Tlemcen Abou-Bekr Belkaid, Tlemcen, Algeria

[2] Higher School of Applied Sciences of Tlemcen (ESSA-T), BP 165 RP Bel Horizon, Tlemcen 13000, Algeria

[3] Civil Engineering Department, Engineering Faculty, Van Yuzuncu Yil University, Van 65080, Turkey

Introduction

The production of new construction materials, such as cementitious composites, has significantly grown during the last few decades. These new materials are mainly based on used construction materials and demolition waste in order to produce recycled concrete aggregates (RCA), which are studied by several researchers in the construction materials field (Muhaiminul et al., 2023; Aligholi & Yıldırım, 2023). The new generation composites based on recycled waste aim to preserve natural resources, reduce health risks related to human and biotic components, recover waste, resolve the

Published online: 18 July 2025

problems of aggregate lack, and finally reduce the environmental issues related to aggregate extraction and disposal of waste, which can also reduce the cost of construction materials as well (Verian et al., 2018). Many types of waste replace natural aggregates (NA) in the literature; the same type of waste can be added to the concrete mixtures as reinforced fiber. For example, authors in (Batayneh et al., 2007) used glass waste as a replacement for fine aggregates; on the other hand, authors in (Arslan, 2016) used the same type of waste as fiber to reinforce concrete. The use of fiber as reinforcement has found applications in civil engineering for years due to its low weight, high strength, and great durability, application in new and corrective constructions. It is increasingly common to use natural fibers as reinforcement. Basalt is a favorable choice for reinforcing concrete and a compelling alternative material. It's high modulus, heat resistance, good resistance to chemical degradation, and excellent shear resistance at the interface (Huazhe, 2019).

The addition of steel fibers to the composition of the concrete makes it more homogeneous and isotropic, transforming it into a ductile material. These fibers help control cracking and change the behavior of the cracked material by bridging the fibers across the cracks (Muneam, 2023). The addition of fiber to concrete provides significant residual strength after cracking, reduces its fragility, increases its ductility, and improves its durability through mechanical reinforcement, thus contributing to the construction of more robust and durable structures. Recent studies (Saha et al., 2024) examined sulphate-resisting cement concrete over portland cement in the presence of salinity. Their finding showed that a small amount of silica fume significantly improved strength, chloride resistance, and microstructural stability.

The experimental and numerical studies related to the impact of RA on the mechanical behavior of cementitious composites have been conducted by several researchers and experts (Hilal, 2016; Pacheco et al., 2019). The authors in (Katkhuda & Shatarat, 2017) presented various experimental tests to improve the performance of using RA. Authors (Fayed & Mansour, 2023) experimentally investigated the performance of sea sand recycled aggregate concrete-filled solid/hollow aluminum tubular columns. The results demonstrated a slight effect of RA on mechanical properties; however, confinement by aluminum tubes significantly enhanced strength, ductility, and stiffness. In this context, special attention was also given to the fracture behavior of RC beams containing RA, due to its influence on crack propagation, ductility, and the fracture mechanism of RC structural elements. The authors in (Guan et al., 2022) report on the flexural behavior of steel FRC based on RA beams through combined experimental and finite element analysis. In the (Guan et al., 2022) paper, the researchers investigated the failure modes, crack development, load-deflection curves, and flexural bearing capacity of the beams. The experimental results are compared to the finite element analysis and indicate that the flexural bearing capacity of steel FRC based RA beams increases with the increase of steel fiber volume fraction and concrete strength, and the decrease of recycled aggregate replacement ratio. Researchers in (Maglad et al., 2023) studied the fracture characteristics of steel fiber-reinforced recycled aggregate concrete experimentally and analytically. The results indicated that the steel fiber-RC made with RA showed similar performance and fracture characteristics compared to normal concrete. Thus, adding steel fibers improved the fracture characteristics, while the brittleness was reduced with increased steel fiber content. (Abdulmajed et al., 2024) Discuss the modeling of the long-term behavior of RC beams made with recycled aggregates, incorporating effects like creep, shrinkage, cracking, and stiffness degradation. The results have a good agreement with experiments and confirm that recycled aggregates can still meet structural serviceability criteria under long-term loading.

Finite element modeling of RA and concrete at macro-, meso-, and micro-scales under static and dynamic loads is the subject of various research projects. For instance, in (Dilbas, 2021a), Dilbas explored the mechanical properties of RAC to characterize its behavior and subsequently modeled a cantilever beam using 3D non-linear FE analysis in ABAQUS, by employing pure plasticity to define RAC properties. Like all digital tools, Abaqus software has many limitations. For example, the experimental data required for integrating unconventional aggregates into the model may be missing or difficult to obtain. To capture the local phenomena, such as cracking or interaction between aggregates, the analyses require a very fine mesh, which can significantly increase the computational cost and may pose convergence problems.

Experimental and numerical tests were conducted by (Mansour et al., 2022). on isolated RC footings, emphasizing the importance of accurately simulating punching shear failure. The results indicated that adding longitudinal reinforcement bars does not affect the punching response of RC isolated footings. However, as the ratio of stirrups increased, an increase in the ultimate load of RC isolated footings was observed.

The high computational time and power requirements, especially for 3D simulations or parametric calculations, are challenging but essential for detailed analysis in such studies. ABAQUS is a powerful tool for investigating the viability of concrete based on unconventional aggregates; however, its success depends on the quality of the input data and the complexity of the model. With sufficient data, Abaqus can provide valuable insights into the optimization

of mixes and the mechanical behavior of innovative materials. A recent study on two-way RC flat slabs by (Ghalla et al., 2024) using 3D nonlinear FE Modeling in ABAQUS to simulate the punching behavior enhanced by internal aluminum reinforcement was validated by experimental results. The validated model was used to investigate the effects of the interspacing between the aluminum sections on the ultimate load, load-deflection responses, stiffness, and absorbed energy of two-way RC flat slabs.

Another experimental and numerical investigations were conducted in (Yang, 2015), on square concrete-filled steel tubes subjected to lateral impact loads. This study aims to examine local damages and failure modes by using non-linear FE modeling and a damaged plasticity model to analyze the concrete behavior. On the other hand, authors in (Dilbas, 2021) mentioned that the falling behavior of materials is usually studied by mathematicians, and the first study was carried out by Comte de Buffon., He experimentally studied the falling of needles (Dilbas, 2021a), thereby discovering the falling behavior of needles, which is controlled by Pi. In his experiments, parallel lines were drawn on a plan. The distance between these lines corresponded to the length of the needles used, which were all the same size. The probability of the needles crossing a line on the plane was expressed as a ratio to Pi. In the study conducted by Dilbas (Dilbas, 2021b), the main objective was to fill a gap in the literature by focusing on the location and behavior of aggregates as they fall into concrete. For this purpose, colored maximum-size marble aggregates are used to visualize their distribution better. Unlike traditional concrete designs, no vibration, manual compaction, or shaking is applied during the casting process to observe the natural behavior of the falling aggregates. These factors should be investigated in further studies, and they are not included in the study conducted by Dilbas (Dilbas, 2021b). However, it is worth studying in the future, and it is a new topic in the literature. The work done in this study is the 3D study of a steel rebar-reinforced concrete beam with and without the addition of RA by the finite element software Abaqus, to study the concrete failure mechanism at the mesoscopic scale taking into account the non-random distribution of aggregates as discussed in the study of Dilbas (Dilbas, 2021b). This method relies on the constant Pi to distribute the aggregates in a non-random manner.

This study aimed to explore the mechanical and failure properties of the reinforced concrete incorporating recycled aggregates with a 20 mm diameter and thickness. It especially focused on understanding the behavior of this material at the mesoscopic scale.

Pi Distribution method and finite element mesoscopic modelling of RC beam

In this part, the failure and mechanical responses of the RC specimen based on RA are studied at a mesoscopic scale by commercial finite element (FE) software (ABAQUS). The distribution of aggregates is carried out according to the PDM to build the structural model of the RC samples at the mesoscopic scale. The PDM is unique because it considers the non-random distribution of aggregates based on the falling aggregate experiment, which simulates the natural process of aggregate placement during concrete casting. Unlike other methods, it accounts for the spatial variation and realistic distribution of aggregates, providing a more accurate representation of the concrete's internal structure and texture. This method was selected for the study based on its emphasis on mesoscopic-scale modeling aligns with the study's focus on understanding the mechanical behavior of RAC. By capturing the inherent heterogeneity of concrete, the PDM allows for a more precise evaluation of the effects of RA and steel reinforcement on properties like ductility, stress redistribution, and overall performance.

To simulate the nonlinear behavior of concrete and recycled aggregate (RA), the Concrete Damaged Plasticity model available in Abaqus (Dassault Systèmes, 2014) was used. This model treats concrete and RA as two separate materials with different mechanical and damage parameters. It accounts for stiffness degradation and plastic deformation under both tensile and compressive loading. The stress-strain behavior is defined by the relationship:

$$\sigma = (1 - d) \, . \, D^{e} : (\epsilon - \epsilon^{p})$$

Where:

σ is the stress tensor,
d is the scalar damage variable,
D^e is the elastic stiffness tensor,
ε is the total strain,
ε^p is the plastic strain.

The plasticity parameters were included in the model, such as dilatation angle, eccentricity, biaxial to uniaxial compressive strength ratio, shape factor, and viscosity parameter. Solid finite elements, also known as continuum FE, are used to model the geometry of the concrete specimen in these current studies.

An isotropically hardened elastoplastic model was used for the steel reinforcement. The plastic deformation, involving a constant strain hardening modulus and a bilinear stress–strain law, which includes an initial linear elastic phase, was used to determine the behavior.

The expression for the yield function is:

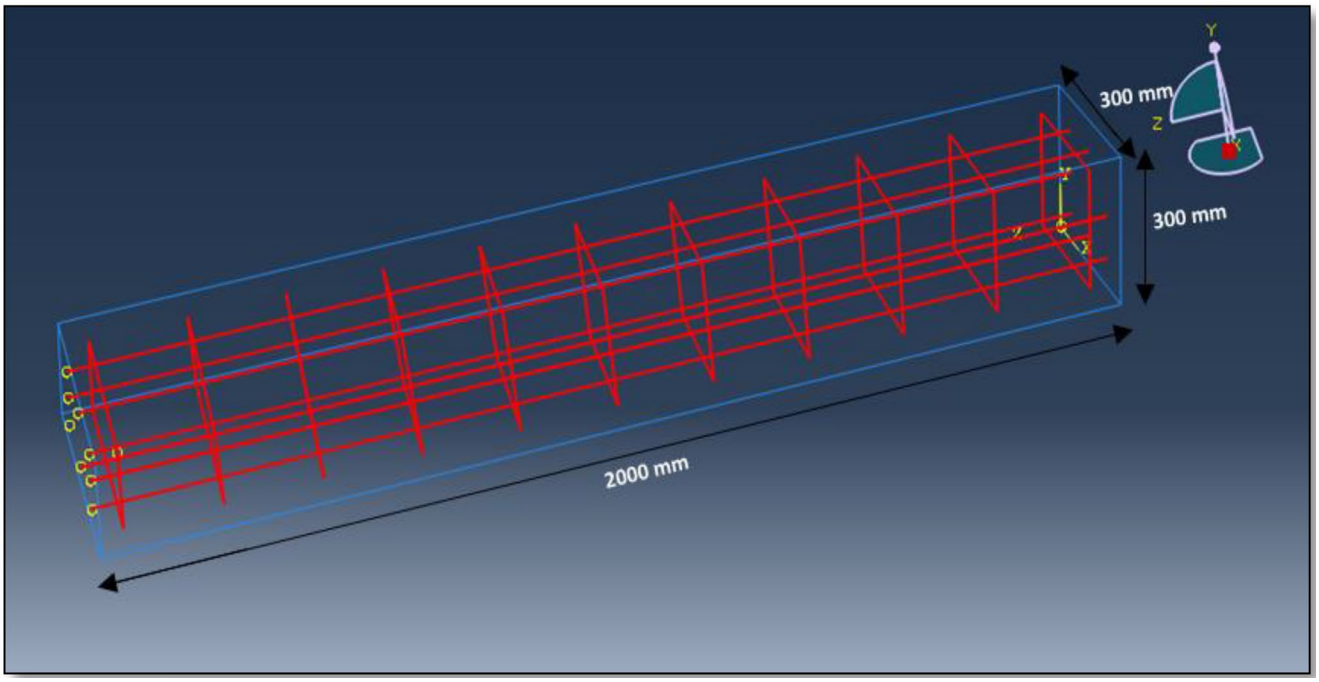

Fig. 1 The geometry of the reinforced concrete beam specimen

Table 1 Mechanical properties of reinforced concrete (RC) beam materials

	Elastic modulus (MPa)	Poisson ratio
RA	10 000	0.20
Steel rebar	205 000	0.30
Concrete	17 585	0.17

Table 2 Concrete damage plasticity of RA

Eccentricity	**Fb0/Fc0**	**K**	**Viscosity Parameter**
0.1	1.16	0.667	0.001
Compressive behavior		**Tensile behavior**	
Yield Stress	**Inelastic Strain**	**Yield Stress**	**Inelastic Strain**
10	0	1	0
8	0.0015	0.05	0.0002
6	0.0025	-	-
4	0.004	-	-

$$f\ (\sigma\ ) = \sqrt{\frac{3}{2}\, s\ :s -\ \sigma_{\,y}\ \leq\ 0}$$

Where:

s is the deviatoric stress tensor

σ_y is the yield stress of the steel

The material is elastic as long as $f(\sigma) \leq 0$, the fibers were represented as bar element embedded in the cement matrix.

Figure 1 shows the geometry of the tested beam, which has a square section of 300 mm depth and 2000 mm overall length. The topological configuration of the longitudinal reinforcement bars and stirrups for this current RC specimen is clearly illustrated in Fig. 1 below.

Table 1 summarizes the mechanical properties of the RC. In this study, one size of aggregate (RA) was used as a cylinder of 20 mm in diameter and depth. RA was used as coarse aggregates by adding them to the concrete using the Concrete Damage Plasticity, as shown in Table 2.

Figure 2 illustrates the boundary conditions of the beam. As shown below, the beam is clamped at its first end, while the other end is subjected to a uniform force in the y direction. The distribution of aggregates was carried out by Dilbas (Dilbas, 2021b). Based on experimental results, this method was proposed to define the locations of the aggregates in the concrete as shown in Fig. 3. The meshing used in this study is 10 mm for all parts of the model. A 3D solid element (C3D8R) was used to model the concrete, which is an 8-node linear brick element, while the fibers are represented as truss elements (T2D2) for all the case studies in this work. these elements are 2-node linear elements with 4 degrees of freedom. The interactions at the interfaces between the mortar matrix-recycled aggregates, and fibers were considered by using the embedded region technique in order to avoid explicitly modeling interfacial contact or cohesive behavior, where the freedom degrees of the embedded nodes are constrained to follow the interpolated motion of the mortar matrix.

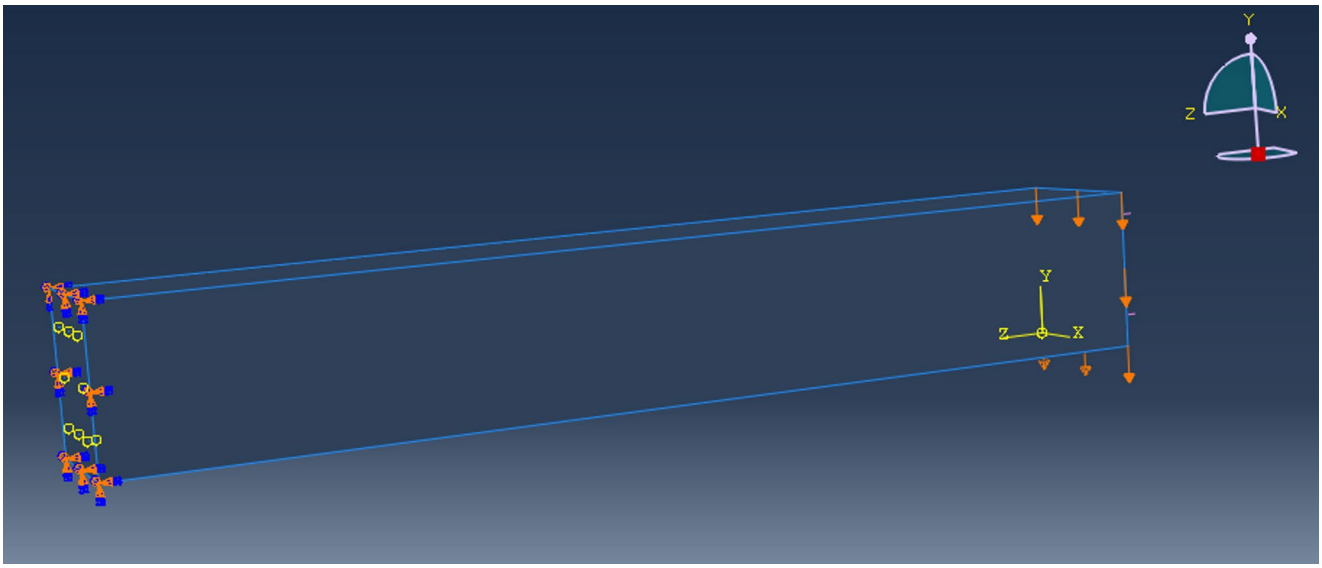

Fig. 2 Boundary conditions and the loading on the beam

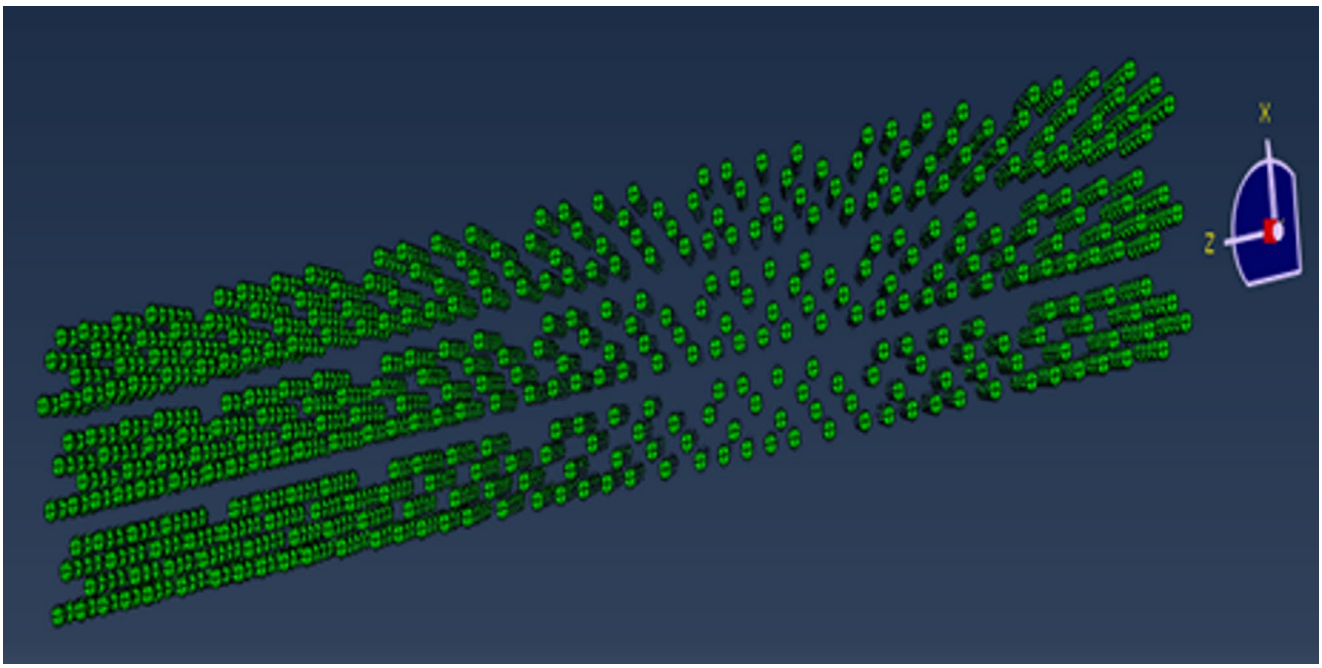

Fig. 3 Pi Distribution of recycled concrete aggregates

Mesoscopic finite element modelling of fiber-reinforced notched beam

In this work, the mesoscopic FE modeling is carried out by the Abaqus to study the failure model and mechanical responses of Fiber-Reinforced notched specimens. The PDM is used to distribute/locate the aggregates to construct the structural model of the mesoscale RC concrete specimen. In this section, notched beams were tested. Figure 4 shows the specimen's geometry size, which has a height of 100 mm, a length of 500 mm, and a negligible depth, featuring a notch of dimensions 10 mm by 30 mm. The mechanical properties of the materials are mentioned in Table 3. Recycled concrete aggregates (RCA) were used as coarse aggregates by adding them to the mortar using the Concrete Damage Plasticity. Details are given in Table 2. In this study authors used three different sizes of RA, such as 5, 10, and 20 mm. Then, steel fibers (10 mm) were incorporated and distributed randomly on the beam.

Considering the symmetry of the specimens, only half of the beam was modeled. The beam is fixed on the left side,

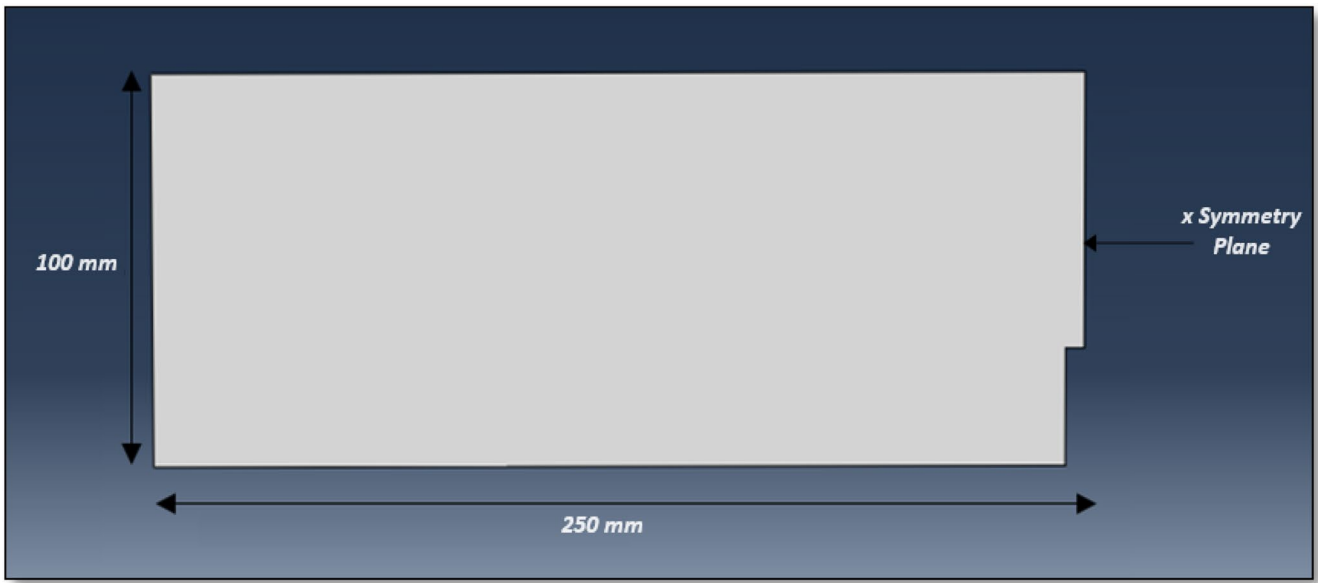

Fig. 4 Geometry of the half-notch specimen

Table 3 Mechanical properties of Fiber reinforced concrete (FRC) beam materials

	Elastic modulus (MPa)	Poisson Ratio
RA	10 000	0.2
Steel Fibers	200 000	0.3
Mortar	40 000	0.15

as shown in Fig. 5. The symmetrical part is also defined as constrained in the « z » direction in this region. The distribution of aggregates was carried out by a simple and complete PDM. This method was proposed based on the results of the tests carried out by (Dilbas, 2021b), to define the locations of the aggregates in the concrete. The meshing of the beam is based on quadrilateral elements, and the FE meshing size is about 6 mm for the entire parts of the model. A mesh sensitivity analysis was conducted to investigate the mesh size sensitivity of the model, using three different mesh sizes, coarse, medium, and fine (2.6 and 12 mm). The bond between the interfaces of the mortar matrix, RA, and the fibers was discretized by using the embedded region at the interaction interfaces, as illustrated in Fig. 6.

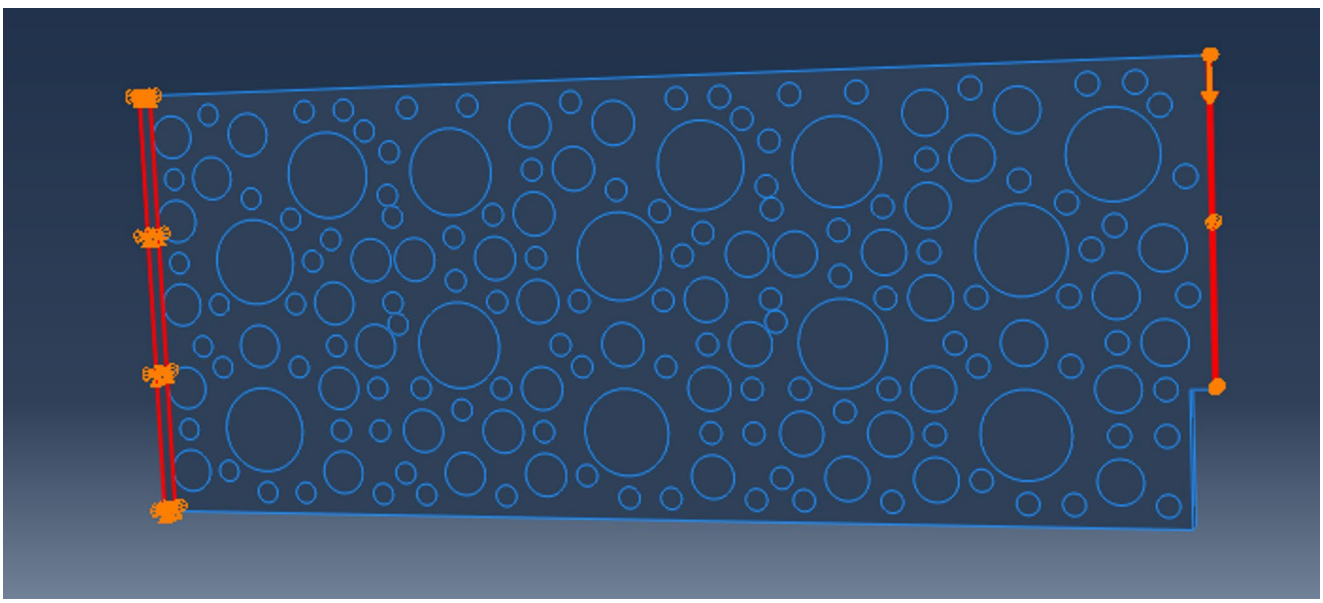

Fig. 5 Boundary conditions and beam loading

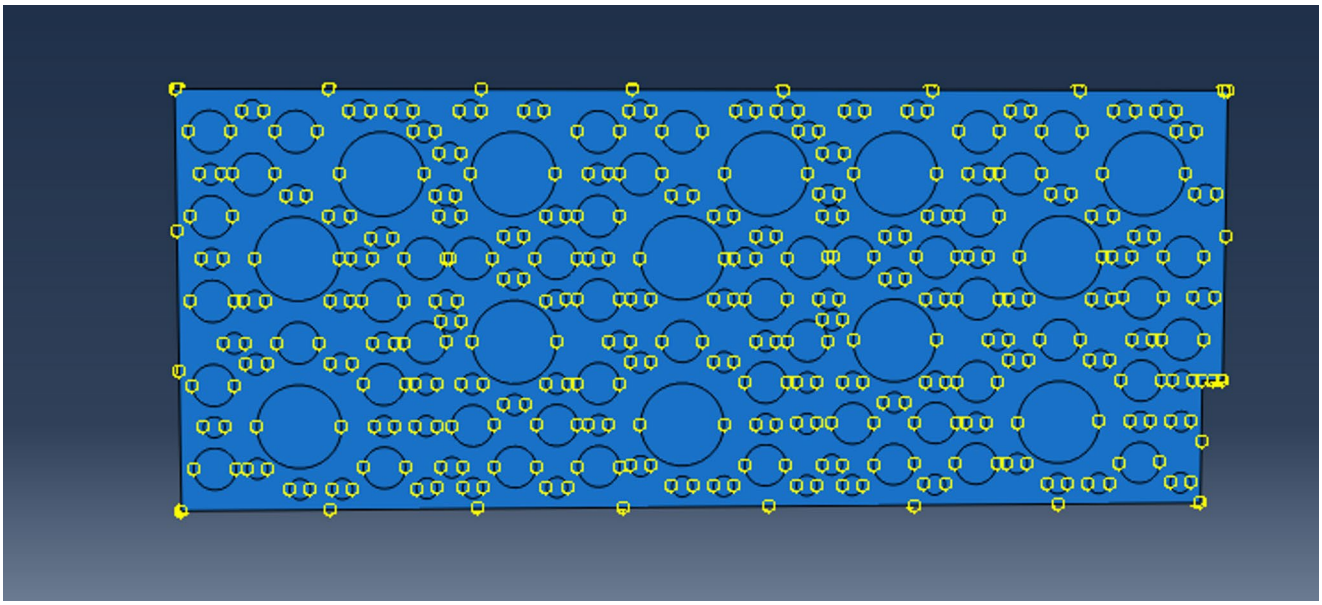

Fig. 6 Interaction between aggregates, fibers, and cement mortar

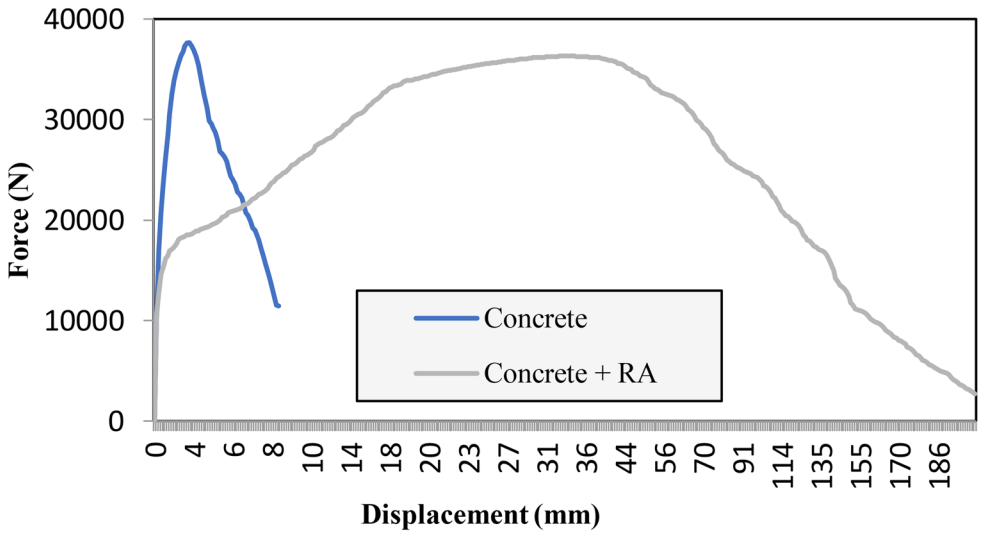

Fig. 7 Load-displacement response of reinforced concrete specimens with and without RA

Results and discussions

As shown in Fig. 7, the linear elastic stiffness of the RAC specimen before the peak load is lower when RA is added to the RC beam due to RA's lower stiffness than NA. The peak load of the specimens is almost the same, with a small difference in the beam with RA due to the low load capacity of RA compared to NA. RA may contain residual mortar from previous use, which can reduce the bond between the aggregate and the cement paste. The reinforced RAC specimen has a higher displacement at peak load than the one with NA. RA has a lower modulus of elasticity than NA due to its high porosity and lower stiffness. It is also ductile, so it can absorb more strain before failure, as shown in Fig. 8.

As shown in Fig. 8 above, the displacement-time curves of RC with and without RA reveal a significant improvement in mechanical behavior due to the inclusion of RA. The curve for concrete with RA (orange) demonstrates a gradual and sustained increase in displacement over time, indicating enhanced ductility and energy absorption capacity. This behavior suggests that the RA contributes to a more distributed stress transfer mechanism, delaying the onset of failure.

In contrast, the curve for concrete without RA (blue) exhibits a steeper and more abrupt increase in displacement, reflecting brittle behavior and limited ductility. This behavior aligns with the expected response of traditional concrete under similar loading conditions, where failure occurs rapidly after reaching the peak stress.

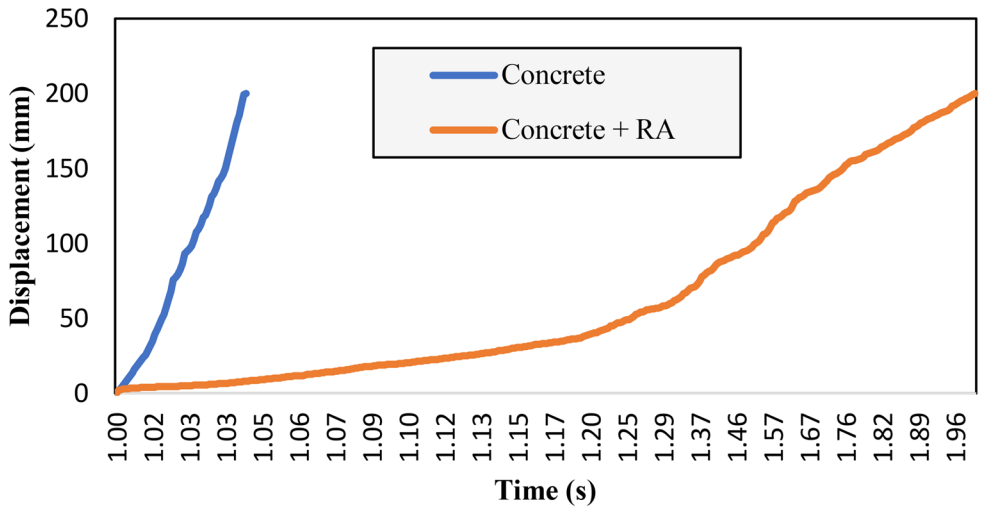

Fig. 8 Displacement-time curves of the reinforced concrete with and without RA

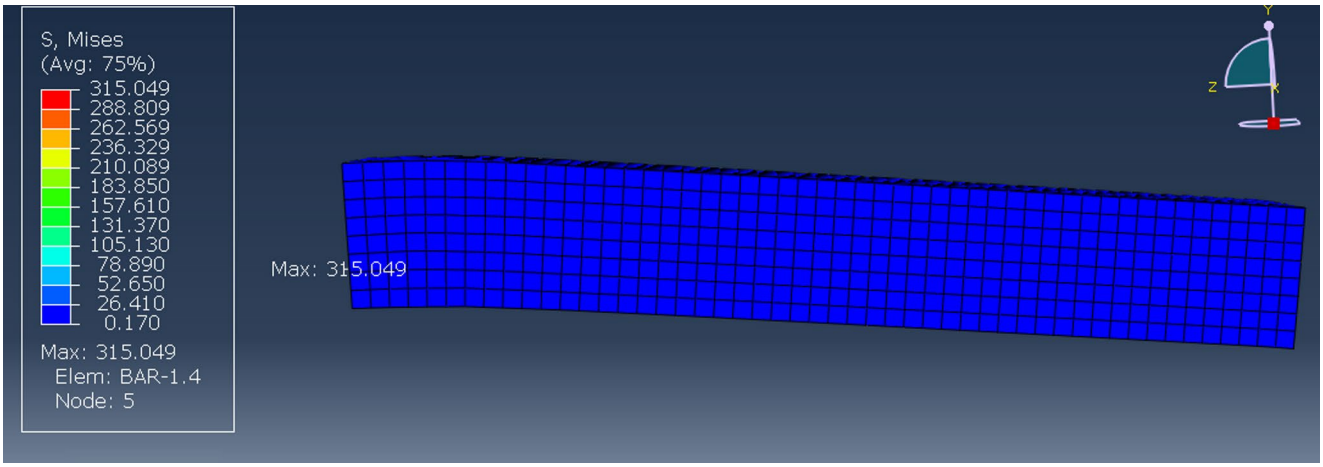

Fig. 9 Von Mises stress distribution in concrete beams with NA

The findings highlight the beneficial role of RA in improving the structural performance of concrete by enhancing its ability to undergo larger deformations before failure. This characteristic is particularly valuable in applications requiring energy dissipation and resilience under dynamic or seismic loading.

The plastic part of the load-displacement curve plays a crucial role in understanding the post-failure behavior of the material. This region of the curve corresponds to the phase in which the concrete continues to deform even after cracking, and it can be seen that the beam with RA has higher values than the beam without RA. These aggregates, acting as additional reinforcement, allow the materials to resist well and, therefore, a significant interaction of the aggregates with the RC.

Figures 9 and 10 compare the Stress Distribution in conventional concrete and RAC beams. The stress distribution in conventional concrete follows the standard bending theory: compression zone (top), neutral zone, and tensile zone (bottom). The change occurs when replacing NA with RA; the high porosity of RA leads to lower compression strength, and the stress transfer is affected by the decrease in stiffness of the mortar matrix, as shown in the figure. the value of the maximum stress is slightly lower in the beam with RA.

Both cases clearly show that the rebars still carried most of the tensile stress; the compressive stress in the case of RA is localized due to the weaker facial bonding.

As shown in Fig. 11, the linear elastic stiffness of the specimens before the maximum force is slightly increased by the addition of fibers. These steel fibers improve the material's response by absorbing part of the applied load and also contribute to the redistribution of stresses more uniformly across the matrix. This can lead to an increase in the linear elastic stiffness of the composite material, meaning it will require a higher force to undergo a given deformation compared to an unreinforced material. The maximum force of the specimens is more remarkable at the peak, the specimen that included RA and steel fiber has a greater maximum load (136 N) compared to that of the specimen that included

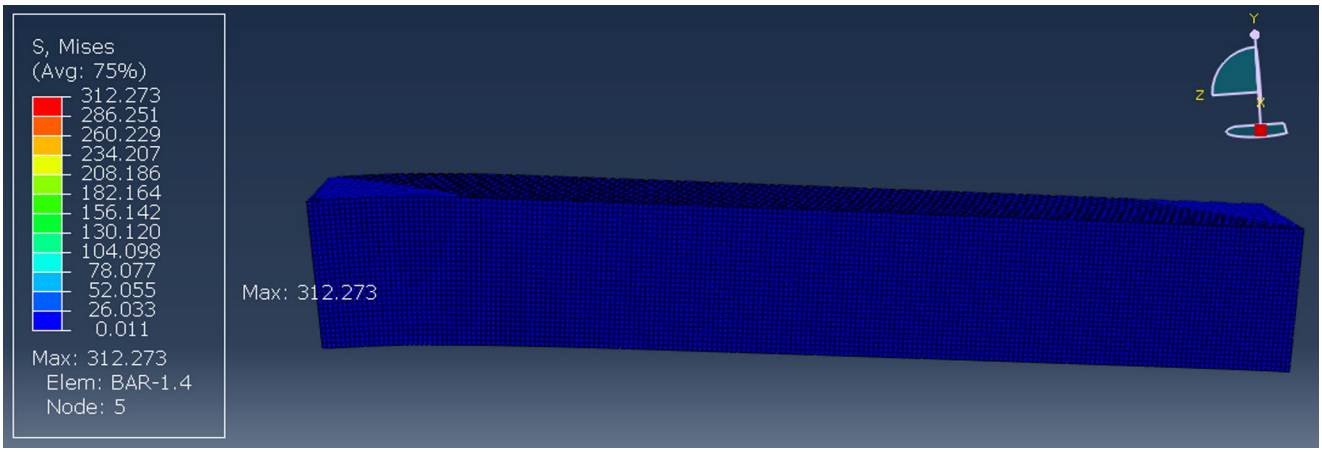

Fig. 10 Von Mises stress distribution in concrete beams with RA

Fig. 11 Load-displacement response of concrete specimens with RA and RA+Fibers

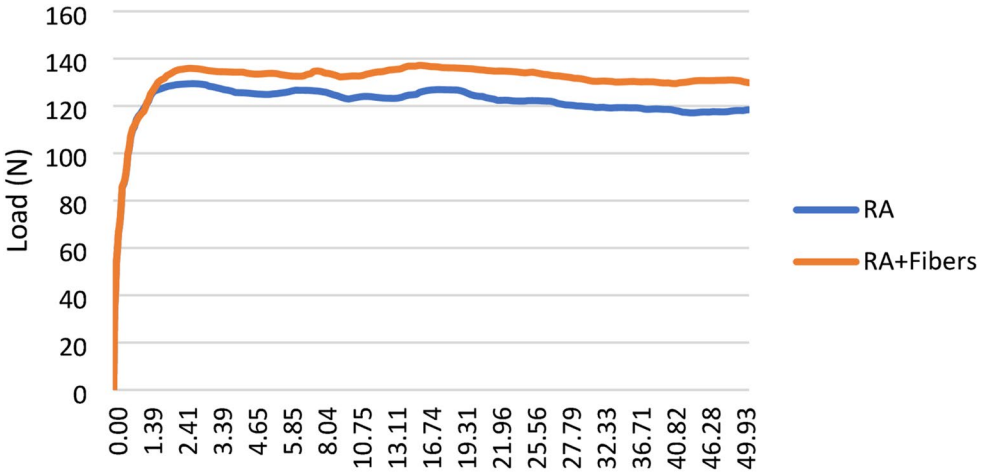

Fig. 12 Load-CMOD response of concrete specimens with RA and RA+Fibers

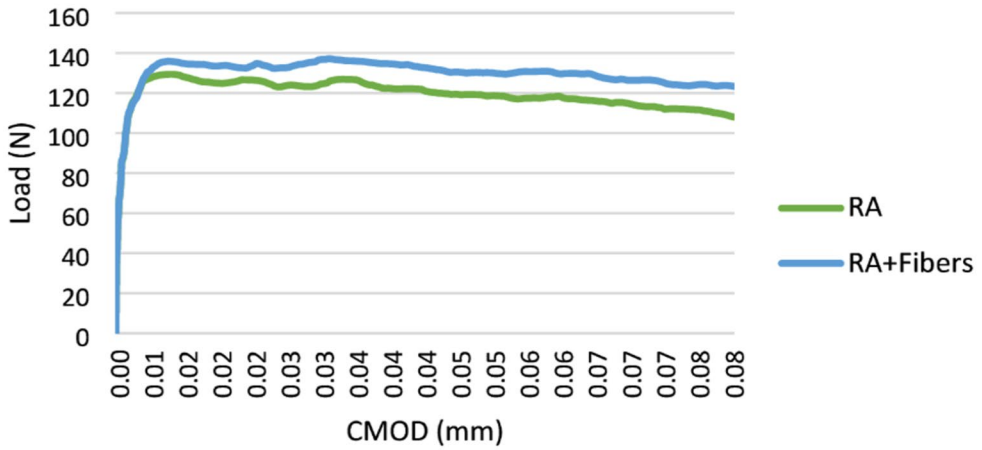

RA (130 N). In the actual figure (Fig. 11), in the plastic part, which plays a crucial role in understanding the post-failure behavior of the material, it is noticed that the fibrous beam has higher bearing values compared to the beam with RA. This region of the curve corresponds to the phase where the concrete continues to deform even after cracks have formed.

The difference between the curves of beams including RA and RA+steel fiber shows that the interaction of the fibers with the mortar matrix is significant. Therefore, the fibers acting as dispersed reinforcements allow the materials to resist well. Figure 12 illustrates the final analysis results in terms of load–CMOD for the specimens with RA and RA+steel fibers. This figure demonstrates that the specimen

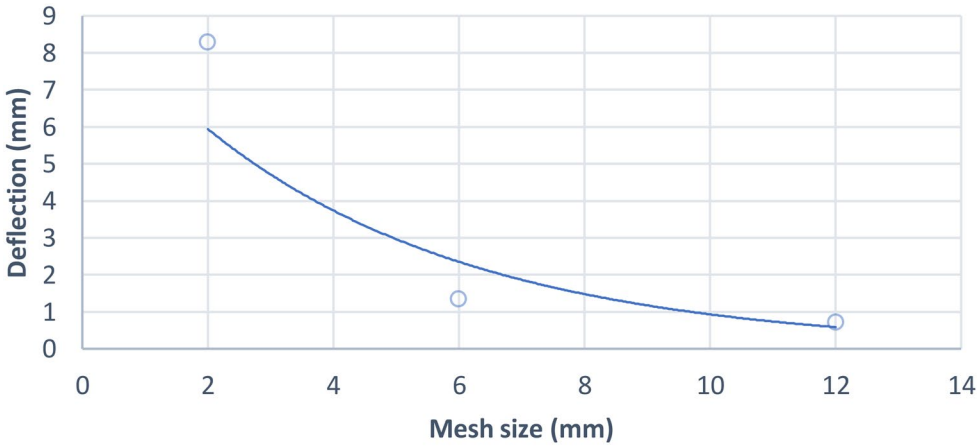

Fig. 13 Deflection-Mesh size curve of concrete specimens with RA

Table 4 Mechanical properties of the beam

Elastic Energy [*N*.mm]	Plastic Energy [*N*.mm]	
	RA	RA+Fibers
64.9	6083.1	6515.6

with RA+steel fibers exhibits a significantly higher load at the peak compared to the specimen with RA. Moreover, the CMOD is higher for the RA+steel fiber sample than for the RA sample. This result is due to the fibers' ability to retain the crack and provide resistance to crack propagation. Therefore, the crack is capable of opening further before final failure occurs.

Adding RA and steel fibers to the concrete composition improves tensile strength due to the elastic nature of the recycled aggregates and steel (Hameed, 2023). In addition, steel fibers can deform before breaking, which allows them to undergo greater deformations before giving way. The attached old cement matrices around the aggregates make the RA a soft material with a porous structure. In contrast, steel fibers have no pores, which means a compact structure (Beddar, 2005). These fibers have a compressive strength greater than that of RA and a relatively large modulus of elasticity compared to RA, which makes them stiffer than RA. Fibers also play a reinforcing role in concrete, which reduces the propagation of cracks under loading, leading to less crack propagation. All of this can lead to more important load-displacement and load-CMOD curves, indicating a better ability of the material to resist loads while maintaining progressive deformation before failing.

The curve in Fig. 13 represents the relationship between mesh size and beam deflection at a load of 120 N, which allows verification of mesh convergence. Indeed, the reduction of mesh size significantly increases the deflection, implying an increased sensitivity of the model to mesh refinement.

The elastic energy and plastic or dissipated energy were calculated by calculating the area under the curve in the elastic region, where the material deforms elastically, and in the plastic region, where the material deforms permanently (CASANOVA, 1995). The results of the elastic and plastic energies for specimens with RA, RA+steel fiber, and the modulus of elasticity are shown in Table 4.

Figures 14 and 15 show the stress distribution in the x and y direction (S11 and S22, respectively) for the specimens that contain RA and RA+steel fiber. It is clear from the Figure that the parts that are subjected to traction have the maximum values of constraint.

The addition of steel fibers contributed to the redistribution and uniformization of stresses along the cross-section of the beam, thus reducing stress concentrations at specific points as shown in Figs. 14(a) and 15(a). In the same figure, it is noted that the max and min values of the stresses are not illustrated on the face of the beam and instead relate to the steel fibers. stresses in steel fibers contribute to their ability to reinforce concrete and improve the beam's performance in terms of strength.

From Fig. 14, we can also notice the stress around the Interfacial Transition Zone (ITZ) between the RA and the mortar, where the stress is greater in some parts than others. The discontinuities at the ITZ may cause stress concentrations and uneven stress distribution in this area.

By plotting the maximum principal plastic strain, which is a good indicator of cracking in tension, clearly shown in Fig. 16, where regions above indicate damage initiation. The red zone shows where strain exceeds the peak.

Conclusion

This paper uses a novel Pi Distribution approach for RA repartition in concrete specimens. The beams are modeled by ABAQUS software on a mesoscopic scale. As a result, the following conclusions were drawn:

- The high porosity of RA aggregates and their weak bond to the cement matrix affect the lower modulus of

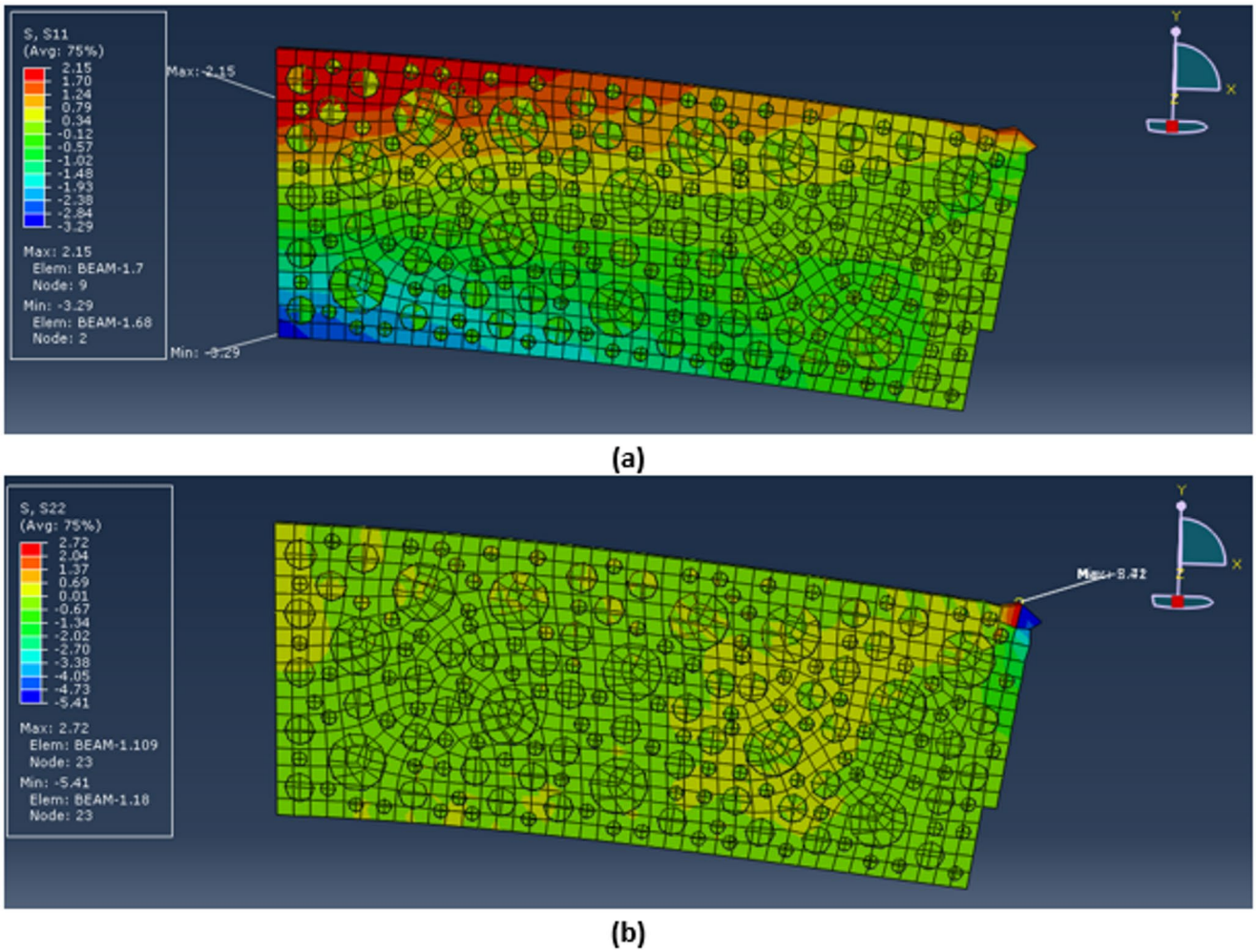

Fig. 14 Stress distribution of concrete specimens with RA in the x direction (**a**) and the y direction (**b**)

elasticity and roundness compared to NA, contributing to greater displacement.

- RA are generally more ductile, so they absorb more stress before failure, which means an increase in displacement at maximum load.
- RA plays a reinforcing role, improving the resistance of materials even after cracking.
- The elastic part of the load-displacement curve for the RAC beam is relatively near the horizontal line (x-axis), but that of natural aggregate concrete is relatively near the vertical line (y-axis) when comparing them.
- The addition of fibers to RA contributes to the increase of the linear elastic stiffness before the maximum force by improving the material's response by absorbing part of the applied load and contributing to the redistribution of stresses more uniformly across the matrix.
- The maximal force of the specimens is more remarkable for RA+steel fiber addition by enhancing the ductility of the concrete due to the significant interaction between the fibers and the concrete.
- Incorporating steel fibers into the concrete affects the plastic part of the curve of load-displacement and load-CMOD. The beam with fibers has higher values of Max Load than the beam with RA, which means the interaction of the fibers with the mortar matrix is significant, and the fibers act as dispersed reinforcement, allowing the materials to resist well.
- The Load-CMOD curves show that the specimen with RA+steel fiber has a significant load at the peak compared to that of RA. Moreover, a greater max CMOD of RA+steel than the specimen with RA is due to the ability to open up further before the breakup, which means the capability of fibers to retain the crack and therefore make the material resist loads while maintaining progressive deformation before failing.
- Steel fibers allow the redistribution and uniformization of stresses all over the beam by absorbing a portion of the stresses and then transmitting it to the material uniformly. The stresses in the steel fibers help to strengthen

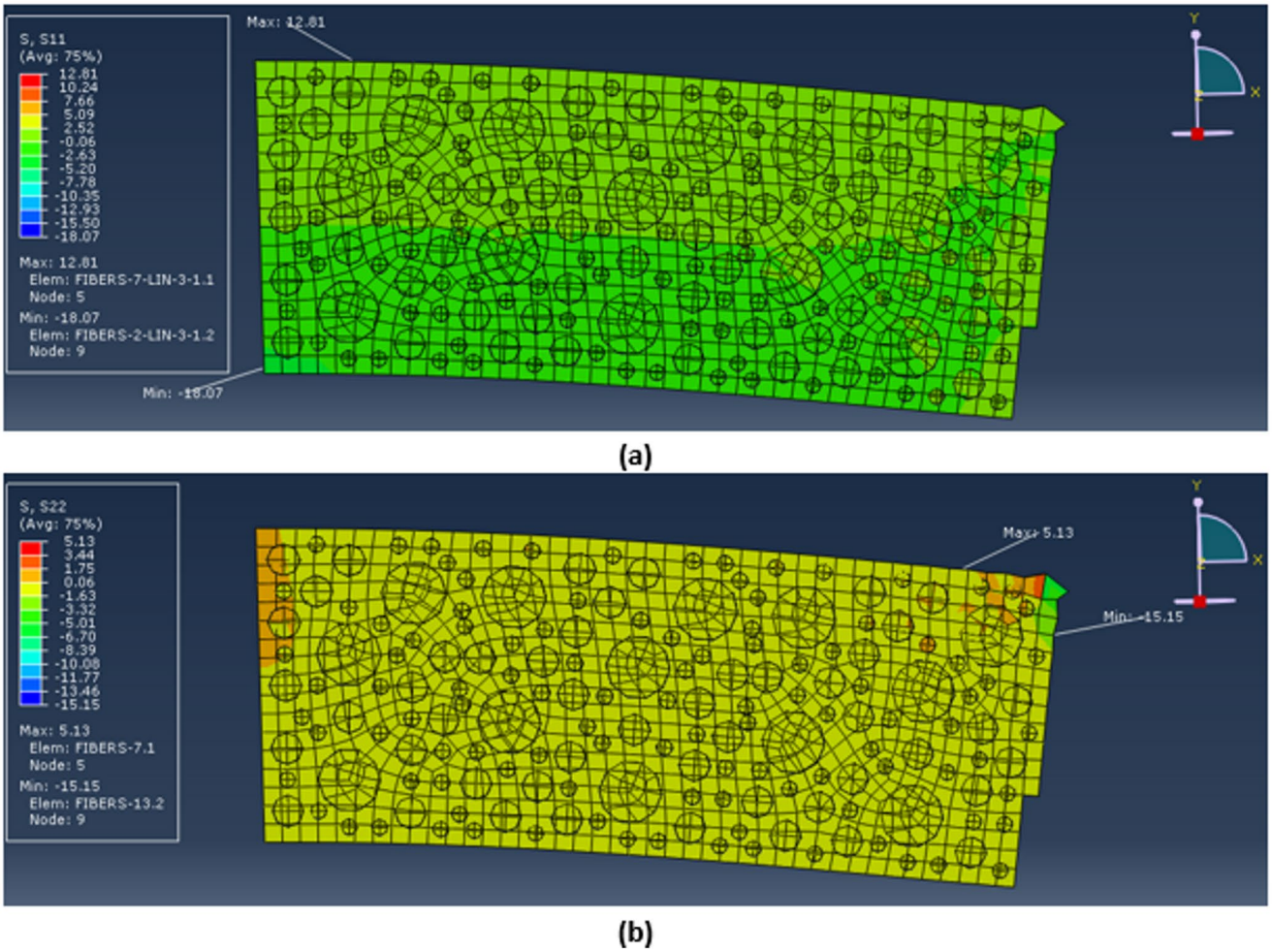

Fig. 15 Stress distribution of concrete specimens with RA+Fibers in the x direction (**a**) and the y direction (**b**)

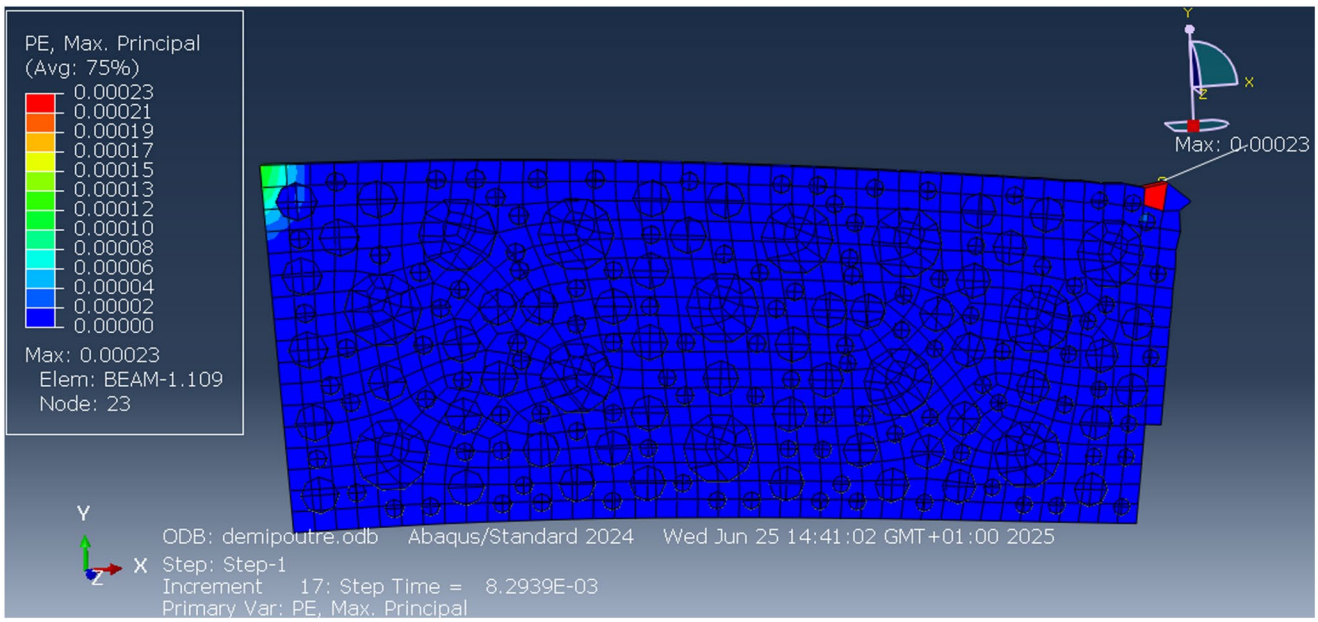

Fig. 16 Failure patterns of the RC beam at the final loading stage

concrete and improve the performance of the beam in terms of resistance.

- The discontinuity of the materials between the mortar and the RA in ITZs can lead to concentration stresses and uneven stress distribution in this area. These discontinuities appear due to different properties of the materials or the slight interaction between the mortar and the RA, leading to localize stress concentrations and potentially affecting the overall structural integrity of the material.

Finally, the main important outcomes of this current numerical study demonstrate the potential of RA to change the mechanical properties of concrete, particularly in terms of ductility and stress redistribution. The use of the PDM provides a more realistic assessment of the aggregate's influence on concrete performance, especially when combined with reinforcement such as steel fibers and rebars. While this study specifically focuses on a certain type of RA, the findings can serve as a foundation for exploring other types of recycled aggregates, such as those obtained from marble waste, tile, and brick waste. Future research should investigate the implementation of these conclusions to a broader range of RA types, including variations in material properties, sizes, and sources, to ensure the relevancy of these results. Besides, other structural elements with many types of aggregates distributed by PDM are the new areas to discover and examine.

Author contributions Meryem Charef and Nabil Kazi Tani; Data curation, Meryem Charef; Formal analysis, Meryem Charef; Investigation, Meryem Charef; Methodology, Hasan Dilbas; Resources, Meryem Charef; Software, Meryem Charef; Supervision, Nabil Kazi Tani and Hasan Dilbas; Validation, Nabil Kazi Tani and Hasan Dilbas; Visualization, Hasan Dilbas; Writing– original draft, Meryem Charef; Writing– review & editing, Nabil Kazi Tani and Hasan Dilbas.

Funding The authors declare that no funds, grants, or other support were received during the preparation of this manuscript.

Data availability No datasets were generated or analysed during the current study.

Declarations

Competing interests The authors declare no competing interests.

References

Abdulmajed, D. A. A., Daud, S. A., & Alrshoudi, F. (2024). Numerical validation of Long-Term behavior of reinforced recycled aggregates concrete beam. *Civ Environ Eng*, *20*(2), 1129–1139. https://doi.org/10.2478/cee-2024-0082

Aligholi, H. Z., & Yıldırım, A. K. (2023). Properties of recycled aggregates and their effects on concrete. *International Journal of Engineering Science*, 7.

Arslan, M. E. (2016). Effects of basalt and glass chopped fibers addition on fracture energy and mechanical properties of ordinary concrete: CMOD measurement. *J Constr Build Mater*, *114*, 383–391. https://doi.org/10.1016/j.conbuildmat.2016.03.176

Batayneh, M., Marie, I., & Asi, I. (2007). Use of selected waste materials in concrete mixes. *J Waste Manag*, *27*, 1870–1876. https://doi.org/10.1016/j.wasman.2006.07.026

Beddar, M. (2005). Permeability and porosity characteristics of steel fiber reinforced concrete. *Asian J Civ Eng*, *6*(4), 317–330.

CASANOVA, P. (1995). Bétons renforcés de fibres métalliques: du matériau à la structure. Etude expérimentale et analyse du comportement de poutres soumises à la flexion et à l'effort trenchant, Ph.D Thesis, l'Ecole Nationale des Ponts et Chaussées, France.

Dassault Systèmes. (2014). *Abaqus Analysis User's Manual, Version 6.14*. Dassault Systèmes Simulia Corp.

Dilbas, H. (2021a). Application of finite element method on recycled aggregate concrete and reinforced recycled aggregate concrete: A review. *J Sustain Const Mater Technol*, *6*, 173–191. https://doi.org/10.14744/jscmt.2021.06

Dilbas, H. (2021b). An Investigation on Aggregate Distribution in Concrete, IJCT, 2 (7), 1–8.

Fayed, S., & Mansour, W. (2023). Structural performance of Seasand recycled aggregate concrete filled solid/hollow aluminum tubular columns: An experimental work. *Structures*, *47*, 1323–1340. https://doi.org/10.1016/j.istruc.2022.12.002

Ghalla, M., Mansour, W., Li, W., Wang, P., Badawi, M., & El Zareef, M. A. (2024). Enhancing the punching performance of twoway RC flat slabs using different configurations of embedded aluminum sections: Experimental program and numerical analysis. *Construction and Building Materials*, *434*, 136737. https://doi.org/10.1016/j.conbuildmat.2024.136737

Guan, Q., Yang, M., Shi, K., & Zhang, T. (2022). Flexural behavior of steel Fiber reinforced recycled aggregate concrete beams. *J Mater*, *15*, 8210. https://doi.org/10.3390/ma15228210

Hameed, R., Maryam, I., Shahzad, S., Hassan, M. I., & Khadija, Arshad, E. (2023). Mechanical performance of 100% recycled aggregate concrete (RAC) bricks. *REV CONSTR Journal*, *22*(1), 203–222. https://doi.org/10.7764/rdlc.22.1.203

Hilal, N. (2016). Characteristics of Self-Compacting Concretes with Tire Rubber Wastes, Ph,D Thesis, University of Gaziantep, Turkey.

Huazhe, J., Yachuang, W., Xinming, C., & Yixuan, Y. (2019). Flexural toughness of basalt Fibre-Reinforced shotcrete and Industrial-Scale testing. *Advances in Materials Science and Engineering*. https://doi.org/10.1155/2019/6568057

Katkhuda, H., & Shatarat, N. (2017). Improving the mechanical properties of recycled concrete aggregate using chopped basalt fibers and acid treatment. *Construction and Building Materials*, *140*, 328–335. https://doi.org/10.1016/j.conbuildmat.2017.02.128

Maglad, A. M., Mansour, W., Tayeh, B. A., Elmasry, M., Yosri, A. M., & Fayed, S. Experimental and analytical investigation of fracture characteristics of steel Fiber-Reinforced recycled aggregate concrete. *Int J Concr Struct Mater* 17.

Mansour, W., Fayed, S., & Basha, A. (2022). *Experimental and numerical analysis of the punching behavior of RC isolated footings*. Steel and Composite Structures. Retrieved June 22, 2025, from http://www.techno-press.org/content/?page=article&journal=scs&volume=45#=5&ordernum=4

Muhaiminul, I. A., & Kazi, A. B. M. M. (2023). Micro-Characterization of recycled concrete aggregate. *J Eng Sci*, *14*(2), 145–155. https://doi.org/10.3329/jes.v14i2.71238

Muneam, A. K., & Makki, R. F. (2023). Shear capacity of reinforced concrete beams with recycled steel fibers. *Open Eng*, *2022-0457*. https://doi.org/10.1515/eng-2022-0457

Pacheco, J., de Brito, J., Chastre, C., & Evangelista, L. (2019). Experimental investigation on the variability of the main mechanical properties of concrete produced with coarse recycled concrete aggregate. *Construction and Building Materials*, *201*, 110–120. https://doi.org/10.1016/j.conbuildmat.2018.12.200

Saha, A., Tonmoy, T. M., Sobuz, M. H. R., Aditto, F. S., & Mansour, W. (2024). Assessment of mechanical, durability and microstructural performance of sulphate-resisting cement concrete over Portland cement in the presence of salinity. *Construction and Building Materials*, *420*, 135527. https://doi.org/10.1016/j.conbuildmat.2024.135527

Verian, K. P., Ashraf, W., & Cao, Y. (2018). Properties of recycled concrete aggregate and their influence in new concrete production. *Resources, Conservation and Recycling*, *133*, 30–49. https://doi.org/10.1016/j.resconrec.2018.02.005

Yang, Y. F., Zhang, Z. C., & Feng, F. (2015). Experimental and numerical study on square RACFST members under lateral impact loading. *Journal of Constructional Steel Research*, *111*, 43–56. https://doi.org/10.1016/j.jcsr.2015.04.004

Publisher's note Springer Nature remains neutral with regard to jurisdictional claims in published maps and institutional affiliations.

Springer Nature or its licensor (e.g. a society or other partner) holds exclusive rights to this article under a publishing agreement with the author(s) or other rightsholder(s); author self-archiving of the accepted manuscript version of this article is solely governed by the terms of such publishing agreement and applicable law.